Gharyan University Journal of Engineering Science (GUJES)
ISSN (3105-4560)
Website: http://journals.gu.edu.ly
email: gujes@gu.edu.ly

# Robust Video Watermarking using Hessenberg Decomposition Blocks Selection Based on the Fourier Transform

Omar Abodena [1*]

[1] Electrical Engineering Department, Faculty of Engineering, University of Gharyan, Gharyan, Libya, omdaina@gmail.com

[*]*Corresponding author:*omdaina@gmail.com

| Received: 08 May 2026 | Accepted: 06 Aug 2026 | Published: 01 Sep 2026 |
|---|---|---|

## Abstract

This study proposes a new robust blind video watermarking technique for copyright protection that combines the Fourier transform, entropy analysis, Hessenberg decomposition, and lifting wavelet transform (LWT). The host video is divided into frames, the RGB channel of each frame is then isolated, and the 2-level LWT is applied to the R channel. The FFT coefficients are divided into 4x4 non-overlapping blocks after the FFT is applied to the high-frequency sub-band of the 2-level LWT. The watermark is then hidden in the first row and first column element of the upper Hessenberg matrix after each selected block has been subjected to Hessenberg decomposition. The proposed technique is extremely invisible with average PSNR=56.421 dB and resilient to attacks with average NC=0.954, as demonstrated by numerous simulated experiments. Comparisons with similar scheme show that the proposed watermarking scheme outperforms the others in terms of invisibility and robustness.

**Keywords**: Fourier transform, entropy analysis, lifting wavelet transform, watermarking, Hessenberg decomposition.

## 1. Introduction

Multimedia data usage has extended, especially in recent years. Multimedia data transfer over computer networks, the internet, cloud services, and Internet of Things devices is one instance of multimedia usage. Because it offers more information than typical text-based data, multimedia data in the form of pictures and videos has grown in popularity recently. The development of inexpensive storage devices and quick communication equipment is another factor contributing to the rise in popularity of image and video usage. In communication, protecting multimedia data becomes crucial. Secret messages or confidential information are frequently included in multimedia data. Numerous methods, including secret sharing and digital watermarking, have been developed to protect multimedia data [1].

A digital watermarking technique inserts a hidden, undetectable signal into a movie that prevents unauthorized users from identifying it. Encrypted watermarks are embedded into multimedia data, and the researcher performs the extraction process to verify the scheme's correctness. Over the last decade, numerous watermarking algorithms have been proposed and categorized according to particular traits [2]. Generally, there are two areas in which video watermarking techniques work: frequency and spatial. By altering the pixels, a watermark is immediately placed in the spatial domain. This domain's methods are computationally simple. However, these schemes are not very resilient and are not very good at robustness. In contrast, frequency domain techniques are essentially effective in this area. The wavelet coefficients of the video frame are combined with the watermark in the frequency domain. The Fourier transform (FT) [3-5], Hadamard transform (HT) [6-8], chirp-z transform [9, 10], discrete cosine transform (DCT) [11-13], Hessenberg decomposition [14-16], LU decomposition [17-19], Schur decomposition [20-22], discrete wavelet transform (DWT) [23-25], and singular value decomposition (SVD) [26-28] are a few of the widely used frequency domain techniques. High payload capacity, imperceptibility, robustness, and increased security are achieved by this domain technique. Furthermore, compared to spatial domain methods, this domain method is computationally costly [29].

A video watermarking method based on the discrete wavelet transform and conventional SVD was presented in the paper [1]. The normalized correlation (NC) value of the extracted watermark under attacks was less than 0.995, and the calculated peak signal-to-noise ratio (PSNR) values for the watermarked videos were less than 40 dB. The study [2] presented a secure video watermarking method that combines graph based transform (GBT), singular valued decomposition (SVD), and hyperchaotic encryption to solve data quality loss. The normalized correlation (NC) value of the recovered watermark was 0.999, and the estimated peak signal-to-noise ratio (PSNR) values for the watermarked video range were less than 37 dB. The paper [29] introduced IGSA-HT (intelligent gravitational search algorithm and hessenberg transform in linear wavelet transform), an ideal keyframe selection-based lossless video watermarking method. The normalized correlation (NC) value of the extracted watermark under attacks was 0.999, while the computed peak signal-to-noise ratio (PSNR) values for the watermarked video range were less than 48.97 dB. The study [13] used a three-dimensional discrete cosine transform (3D-DCT) technique to provide a secure video watermarking system that was extremely resistant to collusion attempts. The average normalized correlation (NC) value of the extracted watermark during image processing and rotation attacks was less than 0.840, and the computed peak signal-to-noise ratio (PSNR) values for the watermarked video range were less than 42.1 dB.

Thus, the three main contributions of the paper are (1) a new proposed video-watermarking technique using lifting discrete transform in combination with fast Fourier transform and Hessenberg transform, to obtain a good performance in terms of invisibility and robustness, (2) the use of entropy analysis to obtain an optimal scaling factor to achieve a balance between imperceptibility and robustness, and (3) the use of a pseudo-random sequence to improve

Gharyan University Journal of Engineering Science (GUJES)
ISSN (3105-4560)
Website: http://journals.gu.edu.ly
email: gujes@gu.edu.ly

scheme security.
The order of the remaining paper is as follows: The next section contains the preliminary steps for the presented method. The presented method is explained in the third section, and the experimental results and discussion are shown in the fourth section. The conclusion is finally drawn in the final section.

## 2. Preliminaries

### 2.1 Lifting Wavelet Transform

Wavelets are tiny waveforms that are used to efficiently and rapidly decorrelate data. Due to its quicker and more effective implementation than the conventional wavelet transform, LWT has emerged as a potent tool for image analysis. In the domains of image compression, watermarking, feature extraction, pattern recognition, and image de-noising, it performs better than standard wavelets. The lifting-based wavelet transformations solve the drawbacks of conventional wavelets by saving time and having a superior frequency localization characteristic. Designing a new wavelet with improved features based on a basic wavelet is the fundamental concept of lifting wavelets [30, 31].

Sweldens divided the wavelet transformation lifting method into three main phases: Split, Predict, and Update. Data is divided into odd and even sets during the split phase. In the predict stage, an odd set is anticipated using an even set. In the high pass, polynomial cancellation is guaranteed by the predict phase. Wavelet coefficients will be used in the update phase to compute the scaling function and modernize the even set.

Split, separates the original signal $x[n]$ into even and odd samples that do not overlap, where $x_e[n]$ for even samples and $x_o[n]$ for odd samples.

$$x_e[n] = x[2n]\,, x_o[n] = x[2n+1] \tag{1}$$

Predict, whether there is a correlation between even and odd samples, as one may predict the other. $x_e[n]$ samples are employed to forecast $x_o[n]$, which are defined as follows:

$$d[n] = x_o[n] - P(x_e[n]) \tag{2}$$

where $P(.)$ is the predictor operator and $d[n]$ is the difference between the actual sample and its predicted value, which is specified as a high-frequency component.

Update, the even samples are updated by using the update operator $U(.)$ and the detail signal $d[n]$. The low-frequency components $l[n]$, which depict the initial signal's approximate form, are then ascertained as follows:

Gharyan University Journal of Engineering Science (GUJES)
ISSN (3105-4560)
Website: http://journals.gu.edu.ly
email: gujes@gu.edu.ly

$$l[n] = x_e[n] + U(d[n]) \tag{3}$$

### 2.2 Fast Fourier Transform (FFT)

The FFT is a computational technique that enables signal analysis, including filter modeling and power spectral analysis, through digital computers. FFT is a very effective method for calculating the DFT of a time series. It utilizes the ability to calculate the DFT's coefficients iteratively, which saves a significant amount of computation time. In addition to cutting down on computing time, the FFT significantly lowers the round-off errors that come with these calculations. The FFT is a sophisticated computer method that generates the DFT coefficients by successively combining progressively bigger weighted sums of input samples [32].

### 2.3 Hessenberg Decomposition

Hessenberg Decomposition [33] is the process of factorizing a generic matrix A using transformations of orthogonal similarity into the form:

$$A = QHQ^T \tag{4}$$

It means that $h_{i\,j} = 0$ whenever $i > j + 1$, that is, when $H$ is an upper Hessenberg matrix, and $Q$ is an orthogonal matrix. Householder matrices are commonly used in the computation of Hessenberg decomposition [34]. The orthogonal matrices of this type constitute the householder matrix ($P$).

$$P = I_n - 2uu^T/u^Tu \tag{5}$$

where $I^n$ is the $n \times n$ identity matrix and $u$ is a non-zero vector in $R^n$. The capacity to add zeros is the primary justification for adopting these matrices. When $A$ is of size $n \times n$, the entire process consists of $n - 2$ steps, further demonstrating the ability to introduce zeros.

$$H = Q^TAQ \;\rightarrow\; A = QHQ^T \tag{6}$$

where $H = A_{n-2}$ and $Q = P_1 P_2 \ldots P_{n-3} P_{n-2}$.

### 2.3 Entropy Analysis

The degree of unpredictability in the image is measured using the entropy. Entropy lists the image's information content. It characterizes the degree of uncertainty or unpredictability present in an image. An image's quality increases with the amount of information it contains. Entropy, often known as Shannon's entropy or entropy of information, quantifies the degree of uncertainty associated with a source of information in the field of information theory [35]. The formula for Shannon's entropy is:

$$E(x) = -\sum p(x) \log p(x) \tag{7}$$

In this case, $p(x)$ represents the potential that '$x$' will appear in picture $E(x)$.

Discrete entropy in image processing refers to the quantity of bits needed to encode picture data. The image will be more detailed if the entropy value is higher.

Gharyan University Journal of Engineering Science (GUJES)
ISSN (3105-4560)
Website: http://journals.gu.edu.ly
email: gujes@gu.edu.ly

# 3. Proposed Method

The two steps of the presented video watermarking technique are watermark embedding, as given in Figure 1, and watermark extraction, as given in Figure 2. The two steps can be expressed as follows:

## 3.1 Watermark Embedding Step

Step Em1: The color video is separated into individual frames.

Step Em2: With $N$ = 1024 and S (number of frames) = 5, a frame $F_{1..s}$ of size $N \times N$ is split into red, green, and blue channels.

Step Em3: The high-frequency subband of the 2-level is chosen after the 2-level LWT is applied to the red channel.

Step Em4: The 2-level LWT's high-frequency subband is subjected to FFT.

Step Em5: FFT coefficients are separated to produce 4×4 non-overlapping blocks, totaling $64^2$.

Step Em6: To get the average of entropy blocks as a scaling factor α, the entropy of each block is computed.

Step Em7: The randperm-function is used to construct pseudo-random sequences with 2-random values based on keys 1 and 2.

Step Em8: Depending on the pseudo-random sequences, the chosen 4×4 blocks are performed by Hessenberg decomposition.

Step Em9: Adjust the magnitudes $M1$ and $M2$ using the binary watermark data $w$

$$if\ w(i,j) = 1, \begin{cases} M_1 = 0.25\alpha \\ M_2 = -0.50\alpha \end{cases} \tag{8}$$

$$if\ w(i,j) = 0, \begin{cases} M_1 = -0.25\alpha \\ M_2 = 0.50\alpha \end{cases} \tag{9}$$

where α is the scaling factor and ($1 \le i,\ j \le$N).

Step Em10: The changed magnitudes $M_1$ and $M_2$ are used to calculate the possible quantization outcomes $T_1$ and $T_2$.

$$T_1 = 2k\alpha + M_1 \tag{10}$$

$$T_2 = 2k\alpha + M_2 \tag{11}$$

where $k$=$floor(ceil(h_{1,1}/\alpha)/2)$, $floor(.)$ indicates the least nearest integer and $ceil(.)$ indicates as the largest nearest integer.

Step Em11: The first-column, first-row component $h_{1,1}$ of the upper Hessenberg decomposition matrix $H$ is chosen as follows to embed the binary watermark:

$$h'_{1,1} = \begin{cases} T_2\ if\ abs\left(h_{1,1} - T_2\right) < abs\ \left(h_{1,1} - T_1\right) \\ T_1\ else \end{cases} \tag{12}$$

where $abs(.)$ denotes the absolute value.

Gharyan University Journal of Engineering Science (GUJES)
ISSN (3105-4560)
Website: http://journals.gu.edu.ly
email: gujes@gu.edu.ly

Step Em12: To obtain the $A'$ watermarked block, replace $h_{1,1}$ with $h'_{1,1}$ and then use the inverse Hessenberg decomposition.

$$A' = QH'Q^T \quad (13)$$

Step Em13: To embed watermark bits, steps Em8–Em12 are repeated.

Step Em14: Merge watermarked blocks.

Step Em15: The modified high-frequency subband is obtained by applying the inverse FFT to merged watermarked blocks.

Step Em16: For obtaining the watermarked red channel, apply the inverse of the 2-level LWT using the modified high-frequency subband.

Step Em17: To obtain the watermarked frame, the channels of watermarked R, G, and B are reconstructed.

Step Em18: To embed watermark data in every frame, repeat steps Em2–Em17.

Step Em19: The watermarked color video is obtained by reconstructing all frames collectively.

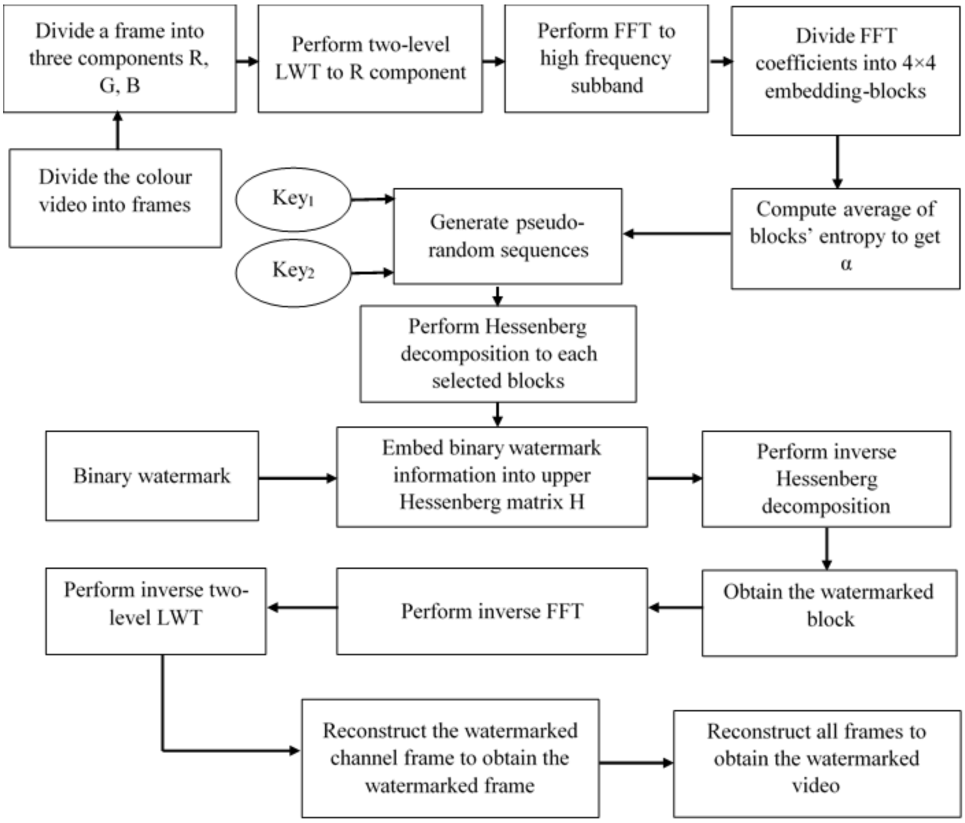


**Figure 1:** The method diagram for watermark embedding

Gharyan University Journal of Engineering Science (GUJES)
ISSN (3105-4560)
Website: http://journals.gu.edu.ly
email: gujes@gu.edu.ly

### 3.2 Watermark Extraction Step

Step Ex1: The watermarked color video is separated into individual frames.

Step Ex2: With $N$ = 1024 and $S$ = number of frames, a watermarked frame $F'_{1..s}$ of size $N\times N$ is split into red, green, and blue channels.

Step Ex3: The high-frequency subband of the 2-level is chosen after the 2-level LWT is applied to the red channel of the watermarked frame.

Step Ex4: The 2-level LWT's high-frequency subband is subjected to FFT.

Step Ex5: FFT coefficients are separated to produce $4\times4$ non-overlapping blocks, totaling $64^2$.

Step Ex6: To get the average of entropy blocks as a scaling factor α, the entropy of each block is computed.

Step Ex7: The randperm-function is used to construct pseudo-random sequences with 2-random values based on keys 1 and 2.

Step Ex8: Depending on the pseudo-random sequences, the chosen $4\times4$ blocks are performed by Hessenberg decomposition.

Step Ex9: Using the first-row, first-column component $h'_{1,1}$ of the upper Hessenberg decomposition matrix $H$, for extracting the binary watermark information as follows:

$$w'_{i,j} = mod\ (\ ceil\left(\frac{h'_{1,1}}{\alpha}\right), 2) \quad (14)$$

where ($1\le i, j\le$N) and $mod(.)$ indicates the modulo operation.

Step Ex10: To extract the watermark bits, steps Ex8–Ex9 are repeated.

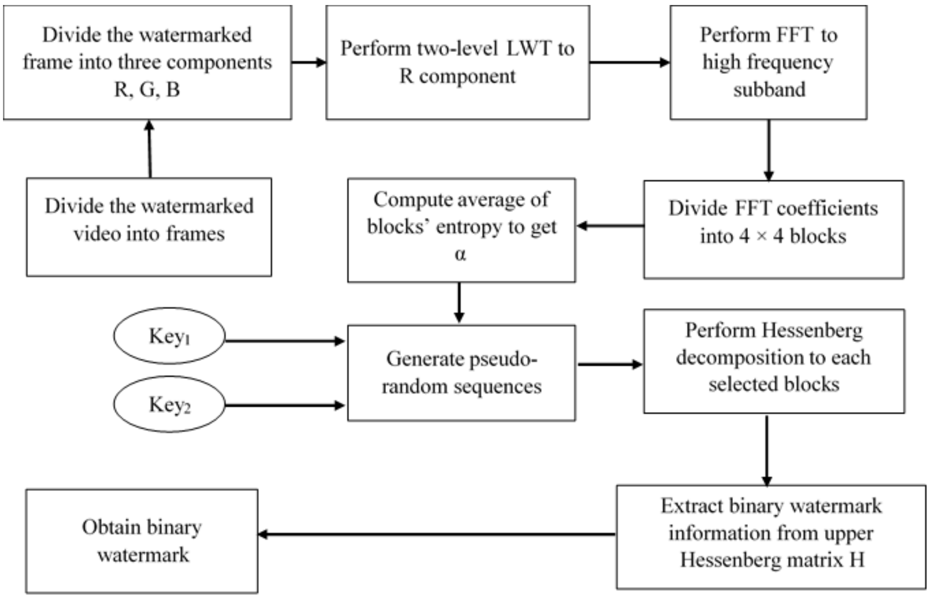


**Figure 2:** The method diagram for watermark extraction

Gharyan University Journal of Engineering Science (GUJES)
ISSN (3105-4560)
Website: http://journals.gu.edu.ly
email: gujes@gu.edu.ly

## 4. Experimental Results and Discussion

Robustness and imperceptibility tests are used to evaluate the effectiveness of the suggested approach. Two objective measures (PSNR and NC) are used in this experiment to assess the performance of the presented scheme by simply judging the presence of the watermark in the host video. Common test color videos are subjected to the suggested color video watermarking approach. As seen in Figure 3, five test color videos [36] referred to as "Akiyo," "Foreman," "News," "Suzie," and "Tennis" are used. Figure 4 displays the three watermarks of size 64×64 used in this scheme.
The *PSNR* value is obtained using the following formula [37]:

$$PSNR = 10\ \log \frac{N_1 \times N_2 \times M \times 255^2}{\sum_{x=1}^{N_1} \sum_{y=1}^{N_2} \sum_{j=1}^{M} [I(x,y,j) - I^*(x,y,j)]^2} dB \tag{15}$$

where $M$ is the number of image channels, $N_1$ and $N_2$ are the number of rows and columns of the host image, $I(x, y, j)$ is the pixel value of the channel $j$ of the host image at the $(x, y)$ location, and $I^*(x, y, j)$ is the pixel value of the channel $j$ of the watermarked image at the $(x, y)$ location.
The *NC* value is obtained using the following formula [13]:

$$NC = \frac{\sum_{x=0}^{I_H-1} \sum_{y=0}^{I_W-1} W_{xy} W'_{xy}}{\sum_{x=0}^{I_H-1} \sum_{y=0}^{I_W-1} (W_{xy})^2} \tag{16}$$

Where $W'_{xy}$ is the extracted watermark pixel value in coordinates *x*, *y*, and $W_{xy}$ is the original watermark's pixel value in coordinates *x*, *y*.
To demonstrate the efficacy of the presented video watermarking scheme in terms of imperceptibility and resilience to attacks, several experiments are conducted.

The following is an explanation of these attacks:
Blurring: The watermarked frames are given a blurring value of 0.5.
Cropping: The top 10% of the collection's watermarked frames are eliminated.
Median filter: The median filter is used to watermarked frames with a 3 × 3 window size.
Gamma correction: A 1.0 gamma adjustment is applied to the watermarked frames.
JPEG 2000 compression: watermarked frames are created using JPEG 2000 compression with a 1 compression ratio.
Salt & pepper noise: The watermarked frames are given a salt & pepper noise value of 0.001.
Scaling: The watermarked frames are enlarged five times.
Sharpening: The watermarked frames are sharpened using a 0.5 quantity value.
Poisson noise: The watermarked frames are subjected to Poisson noise.

Gharyan University Journal of Engineering Science (GUJES)
ISSN (3105-4560)
Website: http://journals.gu.edu.ly
email: gujes@gu.edu.ly


**Figure 3:** The host videos a) Akiyo b) Foreman c) News d) Suzie e) Tennis


**Figure 4:** The watermark images

**Table 1:** The average PSNR values under no attacks

| Host video | Watermark1 | Watermark2 | Watermark3 |
|---|---|---|---|
| **Akiyo** | 62.590 | 62.591 | 62.590 |
| **Foreman** | 54.911 | 54.911 | 54.912 |
| **News** | 55.562 | 55.567 | 55.559 |
| **Suzie** | 62.802 | 62.797 | 62.795 |
| **Tennis** | 46.243 | 46.244 | 46.248 |

**Table 2:** The average NC values under no attacks

| Host video | Watermark1 | Watermark2 | Watermark3 |
|---|---|---|---|
| **Akiyo** | 1.000 | 1.000 | 1.000 |
| **Foreman** | 1.000 | 1.000 | 1.000 |
| **News** | 1.000 | 1.000 | 1.000 |
| **Suzie** | 1.000 | 1.000 | 1.000 |
| **Tennis** | 1.000 | 0.306 | 1.000 |

Gharyan University Journal of Engineering Science (GUJES)
ISSN (3105-4560)
Website: http://journals.gu.edu.ly
email: gujes@gu.edu.ly


**Figure 5:** The watermarked frame and extracted watermark1 under no attack

Each frame's PSNR and NC values are determined separately, and the average of these two parameters is then determined for all video frames. Table 1 and Table 2 summarize the average values of PSNR and NC of the presented method under no attack. As shown in these tables, the quality of the presented watermarked video method is better in terms of invisibility (average PSNR=56.421 dB) and robustness (average NC=0.954).


**Figure 6:** The watermarked frame and extracted watermark2 under no attack


**Figure 7:** The watermarked frame and extracted watermark3 under no attack

Gharyan University Journal of Engineering Science (GUJES)
ISSN (3105-4560)
Website: http://journals.gu.edu.ly
email: gujes@gu.edu.ly

A collection of watermarked video frames and extracted images under no attacks in visual observations is shown in Figures 5 to 7. Tables 3 to 5 represent the average results of robustness after applying various attacks. In visual observations, the figures 8, 10, and 12 illustrate the watermarked video frame (News) after applying several attacks, while figures 9, 11, and 13 illustrate the extracted watermark images after performing various attacks. As seen in these figures, the watermarked video frames are similar to the host video frames, and the extracted watermark images are similar to the original watermark images. The presented watermarking technique performs better in terms of both invisibility and robustness to common attacks, as shown in these tables and figures.

**Table 3:** The average NC values of watermark1 under various attacks

| Attack | Akiyo | Foreman | News | Suzie | Tennis |
|---|---|---|---|---|---|
| **Blurring** | 0.992 | 0.998 | 0.997 | 0.993 | 0.996 |
| **Cropping** | 0.901 | 0.901 | 0.901 | 0.901 | 0.901 |
| **Median filter** | 0.983 | 0.966 | 0.979 | 0.967 | 0.937 |
| **Gamma correction** | 1.000 | 1.000 | 1.000 | 1.000 | 1.000 |
| **JPEG 2000** | 0.285 | 0.998 | 0.999 | 0.320 | 1.000 |
| **Salt & pepper noise** | 0.978 | 0.981 | 0.981 | 0.982 | 0.985 |
| **Scaling** | 1.000 | 1.000 | 1.000 | 1.000 | 1.000 |
| **Sharpening** | 0.996 | 1.000 | 1.000 | 0.999 | 1.000 |
| **Poisson noise** | 1.000 | 1.000 | 1.000 | 1.000 | 1.000 |

**Table 4:** The average NC values of watermark2 under various attacks

| Attack | Akiyo | Foreman | News | Suzie | Tennis |
|---|---|---|---|---|---|
| **Blurring** | 0.985 | 0.997 | 0.997 | 0.987 | 0.997 |
| **Cropping** | 0.933 | 0.933 | 0.933 | 0.933 | 0.253 |
| **Median filter** | 0.982 | 0.958 | 0.974 | 0.957 | 0.915 |
| **Gamma correction** | 1.000 | 1.000 | 1.000 | 1.000 | 0.306 |
| **JPEG 2000** | 0.242 | 0.999 | 0.999 | 0.289 | 1.000 |
| **Salt & pepper noise** | 0.977 | 0.979 | 0.977 | 0.965 | 0.968 |
| **Scaling** | 1.000 | 1.000 | 1.000 | 1.000 | 1.000 |
| **Sharpening** | 0.992 | 1.000 | 0.999 | 0.999 | 1.000 |
| **Poisson noise** | 1.000 | 1.000 | 1.000 | 1.000 | 0.444 |

Gharyan University Journal of Engineering Science (GUJES)
ISSN (3105-4560)
Website: http://journals.gu.edu.ly
email: gujes@gu.edu.ly

**Table 5:** The average NC values of watermark3 under various attacks

| Attack | Akiyo | Foreman | News | Suzie | Tennis |
|---|---|---|---|---|---|
| **Blurring** | 0.988 | 0.999 | 0.998 | 0.993 | 0.996 |
| **Cropping** | 0.957 | 0.857 | 0.857 | 0.857 | 0.857 |
| **Median filter** | 0.982 | 0.956 | 0.977 | 0.963 | 0.931 |
| **Gamma correction** | 1.000 | 1.000 | 1.000 | 1.000 | 1.000 |
| **JPEG 2000** | 0.233 | 0.998 | 0.998 | 0.281 | 1.000 |
| **Salt & pepper noise** | 0.984 | 0.988 | 0.988 | 0.984 | 0.993 |
| **Scaling** | 1.000 | 1.000 | 1.000 | 1.000 | 1.000 |
| **Sharpening** | 0.993 | 1.000 | 0.999 | 0.999 | 1.000 |
| **Poisson noise** | 1.000 | 1.000 | 1.000 | 1.000 | 1.000 |

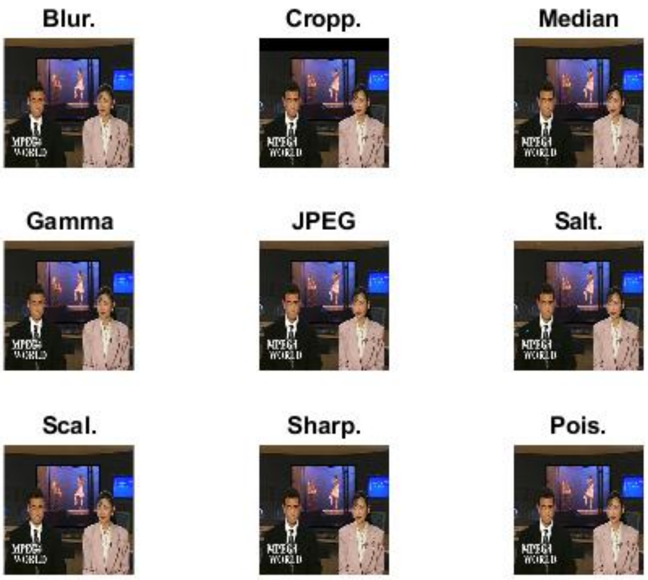


**Figure 8:** The watermarked News frame with watermark1 under various attacks

Gharyan University Journal of Engineering Science (GUJES)
ISSN (3105-4560)
Website: http://journals.gu.edu.ly
email: gujes@gu.edu.ly

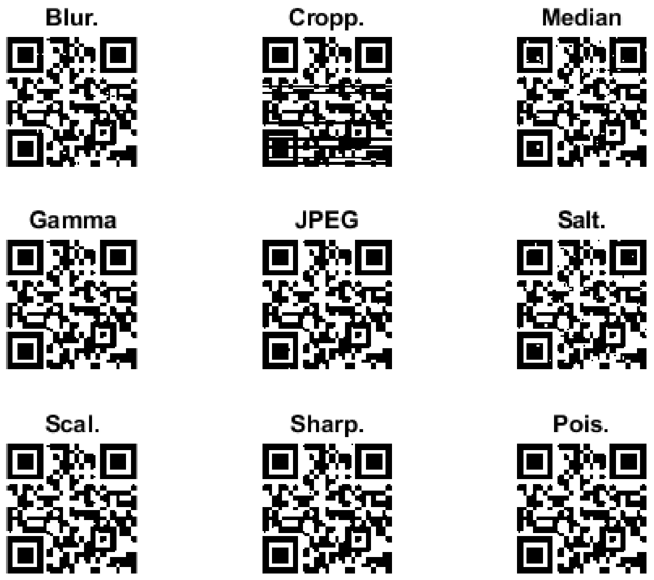


**Figure 9:** The extracted watermark1 of the News frame under various attacks

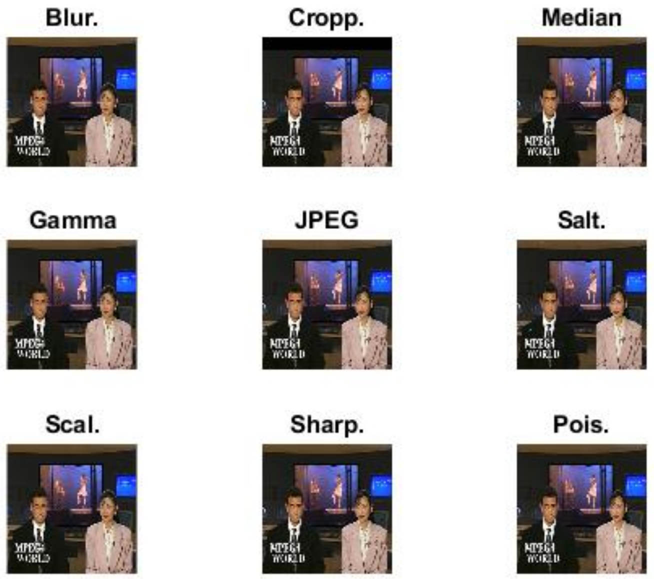


**Figure 10:** The watermarked News frame with watermark2 under various attacks

Gharyan University Journal of Engineering Science (GUJES)
ISSN (3105-4560)
Website: http://journals.gu.edu.ly
email: gujes@gu.edu.ly

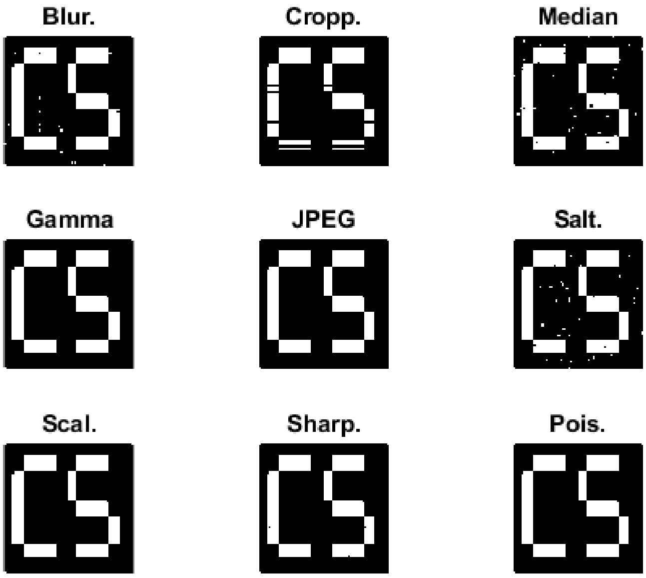


**Figure 11:** The extracted watermark2 of the News frame under various attacks

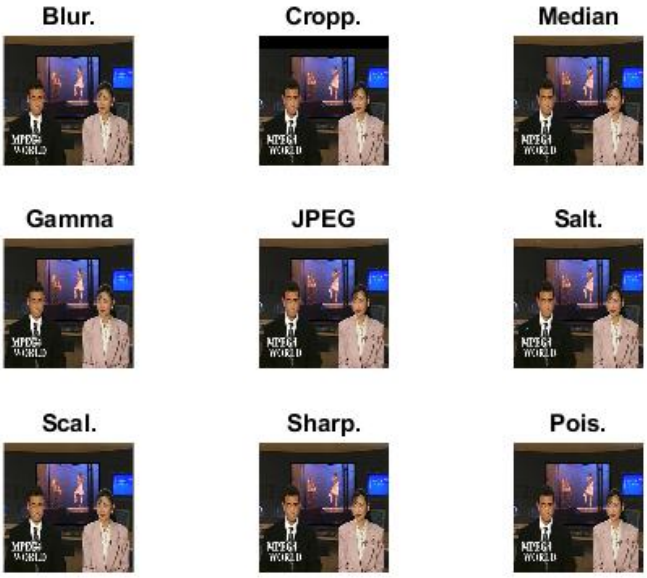


**Figure 12:** The watermarked News frame with watermark3 under various attacks

Gharyan University Journal of Engineering Science (GUJES)
ISSN (3105-4560)
Website: http://journals.gu.edu.ly
email: gujes@gu.edu.ly

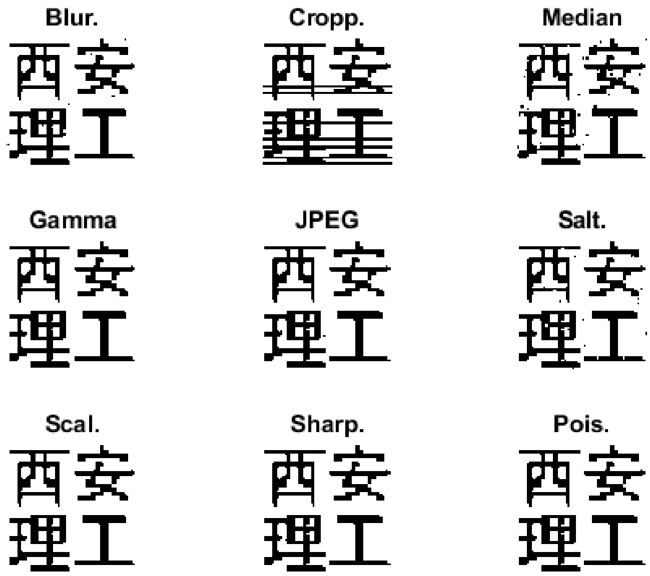


**Figure 13:** The extracted watermark3 of the News frame under various attacks

For further investigation, Table 6 tabulates the evaluation parameters of the comparison between the presented method and the existing method [13] that made use of the same videos and the same watermark image (watermark1). As seen in the table, the presented method provides better results in terms of both invisibility and robustness than the existing method.

**Table 6:** The comparative PSNR and NC results between the proposed method of watermark1 and the existing method

| Host video | Method | PSNR | NC | | |
|---|---|---|---|---|---|
| | | | Poisson noise | Median filter (3*3) | Salt & pepper noise (0.01) |
| Akiyo | Keyvanpour et al. [13] | 41.400 | 0.728 | 0.839 | 0.717 |
| | Proposed | 62.590 | 1.000 | 0.983 | 0.849 |
| Foreman | Keyvanpour et al. [13] | 40.600 | 0.710 | 0.801 | 0.650 |
| | Proposed | 54.911 | 1.000 | 0.966 | 0.878 |
| News | Keyvanpour et al. [13] | 42.100 | 0.719 | 0.820 | 0.687 |
| | Proposed | 55.562 | 1.000 | 0.979 | 0.886 |

Gharyan University Journal of Engineering Science (GUJES)
ISSN (3105-4560)
Website: http://journals.gu.edu.ly
email: gujes@gu.edu.ly

## 5. Conclusion

In this work, a new blind robust watermarking video technique based on the Fourier transform, lifting wavelet transform, Hessenberg decomposition, and entropy analysis is presented. In this scheme, different standard colour videos are utilized to hide different watermarks in order to analyze the effect of different watermarks on different original colour videos. Various digital watermarking attacks are applied including adding noise, filtering, Gamma correction, scaling, cropping, sharpening, blurring, and JPEG 2000 compression attacks. The presented watermarking technique has a good performance in terms of invisibility and robustness to common attacks with average of peak signal to noise ratio (PSNR) value with no attack > 56 dB, and normalize cross-correlation (NC) value with no attack = 0.954. The pseudo-random sequence improves the security of the presented scheme. Furthermore, the scaling factor makes the proposed scheme more robust. The proposed method offers superior robustness and invisibility compared to the existing method. The future work can be carried out from the proposed digital watermarking scheme that a colour video digital watermarking scheme should be improved to hide colour image watermark in order to achieve high capacity.

## References

[1] H. Prasetyo, C.-H. Hsia, and C.-H. Liu, "Vulnerability attacks of SVD-based video watermarking scheme in an IoT environment," *IEEE Access*, vol. 8, pp. 69919-69936, 2020.

[2] C. Sharma, B. Amandeep, R. Sobti, T. K. Lohani, and M. Shabaz, "A secured frame selection based video watermarking technique to address quality loss of data: combining graph based transform, singular valued decomposition, and hyperchaotic encryption," *Security and Communication Networks*, vol. 2021, no. 1, p. 5536170, 2021.

[3] O. Abodena, M. Agoyi, and E. Celebi, "Hybrid technique for robust image watermarking using discrete time fourier transform," in *2017 25th Signal Processing and Communications Applications Conference (SIU)*, 2017: IEEE, pp. 1-4.

[4] E. Salah, K. Amine, K. Redouane, and K. Fares, "A Fourier transform based audio watermarking algorithm," *Applied Acoustics*, vol. 172, p. 107652, 2021.

[5] Y.-M. Li, D. Wei, and L. Zhang, "Double-encrypted watermarking algorithm based on cosine transform and fractional Fourier transform in invariant wavelet domain," *Information Sciences*, vol. 551, pp. 205-227, 2021.

[6] S. Chen, Q. Su, H. Wang, and G. Wang, "A high-efficiency blind watermarking algorithm for double color image using Walsh Hadamard transform," *The Visual Computer*, vol. 38, no. 6, pp. 2189-2205, 2022.

[7] A. Dash, K. Naik, and P. Priyadarshini, "Enhancing copyright protection with Hadamard transform-based blind digital watermarking using the cycling chaos system," *International Journal of Computers and Applications*, pp. 1-14, 2024.

[8] Z. Liu, X. Chen, C. Shi, G. Wang, and Q. Su, "Enhancing Robustness and Invisibility of Color Image Watermarking Through Discrete Hankel and Hadamard Transforms," *Circuits, Systems, and Signal Processing*, vol. 44, no. 12, pp. 9484-9511, 2025.

[9] O. Abodena, "Robust and high-capacity audio watermarking basedon chirp z-transform," in *2021 29th Signal processing and communications applications conference (SIU)*, 2021: IEEE, pp. 1-4.

[10] M. Agoyi, E. Çelebi, and G. Anbarjafari, "A watermarking algorithm based on chirp z-transform, discrete wavelet transform, and singular value decomposition," *Signal, Image and Video Processing,* vol. 9, pp. 735-745, 2015.

[11] M. Begum, J. Ferdush, and M. S. Uddin, "A Hybrid robust watermarking system based on discrete cosine transform, discrete wavelet transform, and singular value decomposition," *Journal of King Saud University-Computer and Information Sciences,* vol. 34, no. 8, pp. 5856-5867, 2022.

[12] N. Agarwal and P. K. Singh, "Discrete cosine transforms and genetic algorithm based watermarking method for robustness and imperceptibility of color images for intelligent multimedia applications," *Multimedia tools and applications,* vol. 81, no. 14, pp. 19751-19777, 2022.

[13] M. R. Keyvanpour, N. Khanbani, and M. Boreiry, "A secure method in digital video watermarking with transform domain algorithms," *Multimedia Tools and Applications,* vol. 80, no. 13, pp. 20449-20476, 2021.

[14] D. Awasthi and V. K. Srivastava, "Hessenberg decomposition-based medical image watermarking with its performance comparison by particle swarm and JAYA optimization algorithms for different wavelets and its authentication using AES," *Circuits, Systems, and Signal Processing,* vol. 42, no. 8, pp. 4953-4984, 2023.

[15] O. Abodena, "A robust blind watermarking scheme based on lifting wavelet transform and hessenberg decomposition," *Journal of Pure & Applied Sciences,* vol. 21, no. 2, pp. 48-54, 2022.

[16] F. Hu, H. Cao, Q. Su, G. Wang, and T. Yao, "EBOF: A fusion-domain color image watermarking scheme based on approximate Hessenberg factorization," *Optik,* vol. 287, p. 171084, 2023.

[17] N. Phuong Thi and T. Ta Minh, "A new block selection strategy from LU decomposition domain for robust image watermarking," *Multimedia Tools and Applications,* vol. 83, no. 7, pp. 19301-19325, 2024.

[18] O. Abodena, "An Optimized Image Watermarking Technique Based on LU Factorization and Entropy Analysis," *AL-JAMEAI,* vol. 39, no. 2, pp. 21-38, 2024.

[19] D.-O. Muñoz-Ramírez, B.-P. García-Salgado, V. Ponomaryov, R. Reyes-Reyes, S. Sadovnychiy, and C. Cruz-Ramos, "A color image watermarking framework for copyright protection of stereo images based on binocular just noticeable difference and LU decomposition," *Multimedia Tools and Applications,* vol. 80, pp. 13707-13734, 2021.

[20] P. Liu, H. Wu, L. Luo, and D.-S. Wang, "DT CWT and Schur decomposition based robust watermarking algorithm to geometric attacks," *Multimedia Tools and Applications,* vol. 81, no. 2, pp. 2637-2679, 2022.

[21] O. Abodena, "A Robust Blind Grayscale Image Watermarking Technique Based on Schur Decomposition and Entropy Analysis," *University Gharyan Journal,* vol. 28, no. 2, pp. 471-493, 2023.

[22] K. Prabha and I. Shatheesh Sam, "Lifting Scheme and Schur Decomposition based Robust Watermarking for Copyright Protection," in *Intelligent Systems: Proceedings of SCIS 2021*, 2021: Springer, pp. 143-151.

Gharyan University Journal of Engineering Science (GUJES)
ISSN (3105-4560)
Website: http://journals.gu.edu.ly
email: gujes@gu.edu.ly

[23] R. K. Batchu, T. V. R. Pranay, M. R. Dontha, S. K. R. Dasarapu, A. Avinash, and A. Bhima, "Securing medical images with PCA-DCT-DWT watermarking for tamper detection and self-recovery," *Quality & Quantity,* pp. 1-58, 2026.

[24] J. Ferdush, M. Begum, and M. S. Uddin, "A machine-learning and GA-optimized encrypted LL $$ _3 $$ watermarking scheme in the DWT domain," *Multimedia Tools and Applications,* vol. 85, no. 6, p. 546, 2026.

[25] V. Sabeti, "An enhanced dwt-svd-based robust image watermarking scheme optimized for imperceptibility and robustness," *Arabian Journal for Science and Engineering,* vol. 50, no. 19, pp. 15529-15550, 2025.

[26] B. Amira and F. Lazhar, "A randomized block-based SVD image watermarking technique for IoT applications," *Multimedia Tools and Applications,* vol. 85, no. 1, p. 39, 2026.

[27] J. Zhang, X. Xi, J. Du, and C. Qu, "DCT-SVD based hybrid frequency domain watermarking for remote sensing images in the 3D wavelet domain," *Circuits, Systems, and Signal Processing,* vol. 45, no. 3, pp. 2000-2029, 2026.

[28] S. Priyadharsini and A. Kanhe, "A hybrid Chebyshev-SVD based approach for robust audio watermarking application," *Signal Processing,* p. 110279, 2025.

[29] R. Singh, H. Mittal, and R. Pal, "Optimal keyframe selection-based lossless video-watermarking technique using IGSA in LWT domain for copyright protection," *Complex & Intelligent Systems,* vol. 8, no. 2, pp. 1047-1070, 2022.

[30] P. Pal, P. Chowdhuri, and T. Si, "A novel watermarking scheme for medical image using support vector machine and lifting wavelet transform," *Multimedia Tools and Applications,* vol. 82, no. 26, pp. 41187-41206, 2023.

[31] H. Agarwal and F. Husain, "Development of payload capacity enhanced robust video watermarking scheme based on symmetry of circle using lifting wavelet transform and SURF," *Journal of Information Security and Applications,* vol. 59, p. 102846, 2021.

[32] W. T. Cochran *et al.*, "What is the fast Fourier transform?," *Proceedings of the IEEE,* vol. 55, no. 10, pp. 1664-1674, 1967.

[33] O. Abodena and M. Agoyi, "Colour image blind watermarking scheme based on fast walsh hadamard transform and hessenberg decomposition," *Studies in Informatics and Control,* vol. 27, no. 3, pp. 339-348, 2018.

[34] G. Bhatnagar, Q. J. Wu, and B. Raman, "Biometric template security based on watermarking," *Procedia Computer Science,* vol. 2, pp. 227-235, 2010.

[35] S. Kumar and B. K. Singh, "Entropy based spatial domain image watermarking and its performance analysis," *Multimedia Tools and Applications,* vol. 80, no. 6, pp. 9315-9331, 2021.

[36] C. Montgomery. "Xiph. org Video Test Media (derf's collection), the xiph open source community, 1994." https://media.xiph.org/video/derf/ (accessed Febraury, 2019).

[37] B. Bao and Y. Wang, "A robust blind color watermarking algorithm based on the Radon-DCT transform," *Multimedia Tools and Applications,* vol. 83, no. 24, pp. 64663-64682, 2024.